Journal of Interfaces, Thin films, and Low dimensional systems 4 (2) Winter and Spring (2021) 365-378

An evaluation for CIGS based thin-film solar cells development

Review paper

Mojtaba Jamiati*

Department of Physics, Naragh Branch, Islamic Azad University, Naragh, Iran

ARTICLE INFO

Article history:
Received 14 March 2021
Revised 20 November 2021
Accepted 20 November 2021
Available online 8 December 2021

Keywords:
Solar cell
CIS
CIGS
Thin film
Photovoltaic

ABSTRACT

Thin film solar cells are desirable due to minimal material usage, cost effective synthesis processes, and a promising trend in efficiency rise. This review summarizes the current status of chalcopyrite $\mathrm{Cu(InGa)(S,Se)_2}$ (CIGS) thin film solar cell technology with a focus on recent advancements and emerging concepts intended for higher efficiency and novel applications. The recent developments and trends of research in laboratory and industrial achievements communicated within the last years are reviewed and the major developments linked to alkali post deposition treatment and composition grading in CIGS, surface passivation, buffer and transparent contact layers are emphasized. In recent years, a lot of effort has been initiated to develop low-cost thin-film solar cells, which are alternatives to high-cost silicon (Si) solar cells. Copper Indium Gallium Selenide (CIGS) based solar cells have become one of the most promising candidates among the thin film technologies for solar power generation. The current record efficiency of CIGS has reached 22.6%, which exceeds the current multi crystalline Si record efficiency (21.9%). However, material properties and efficiency on small area devices are crucial aspects to be considered before manufacturing into large scales. Chalcopyrite-based solar cells were first developed using $\mathrm{CuInSe_2}$ absorber material, but it quickly became dependent on the $[\mathrm{Ga/(In+Ga)}]$ ratio. CIGS and related alloys are a direct band gap semiconductor with high efficiency, low cost, large absorption coefficient, and very good stability in outdoor tests.

1 Introduction

At the beginning of the 21^{st} century, numerous different energy sources were used to satisfy the World's need for electricity. The sunlight is one of the largest energy sources in nature. However, so far human has not been able to provide a large share of his energy from this source. Hence, in recent decades, extensive efforts have been done in solar cells modeling and fabricating to use this energy. In order to convert this energy to a usable form, special absorbent materials are needed, which (1) have optimum bandgap to sunlight energy and (2) are not harmful to the environment [1]. The sun is the most abundant source of renewable energy to meet up the present and future global energy demands in terawatt (TW) scale deployment. In this direction, solar cell is one of the best possible means for directly converting sunlight into usable energy without producing any harmful by products. In general, there are two approaches for the conversion of harvested sunlight into electricity, namely single junction and multi junction solar cells.

Among all types of solar cells, second generation thin film cells are favorable because of their low cost material usage and promising trend in efficiency rise. Although first generation silicon (Si) solar cells are still dominant players in photovoltaic (PV) literatures, Silicon (Si) solar cells dominate the PV market (92%) followed by cadmium telluride

*Corresponding author.
Email address: drmjamiati@Gmail.com

DOI: 10.22051/jitl.2022.35435.1051

(CdTe, 5%), copper indium gallium selenide ($\mathrm{CuInGaSe_2}$ or CIGS, 2%) and amorphous silicon (a-Si:H, ~1%). Si wafer with thickness around 180μm is the traditional material being used for module manufacturing and it has attained significant level of maturity at the industrial level. Its production cost is a major concern for energy applications. About 50% of the cost of Si solar cell production is due to Si substrate while device processing and module processing accounts for 20% and 30% respectively [2].

Alternate to Si solar cells are thin film solar cells fabricated on glass substrates. The main demerits of using glass substrates are fragile nature of modules, cost of glass wafer having thickness of 300–400μm, and low specific power (kW/kg) etc. Specific power is an important factor when solar cells are used in space applications. A high specific power exceeding 2 kW/kg can be achieved by flexible solar cells on polymer films which is useful for terrestrial as well as space applications. Production cost can be lowered by using flexible substrates and roll-to-roll production (R2R) technique. However, flexible solar cell technology is less mature when compared to the cells fabricated on rigid substrate counterparts. Due to four main requirements - high efficiency, low-cost production, and high throughput and high specific power, a major research and development focus has been shifted towards flexible solar cells. It can offer a unique way to reach terawatt scale installation by using the high throughput R2R fabrication technique [3].

The process of cost reduction in non-Si thin-film solar cells is easier than Si solar cells. We can obviously improve the performance of thin solar cells whereas the parameters connected with Si solar cell efficiency are not capable to be enhanced. The main drawback with the Si solar cells is that it is an indirect band gap semiconductor and needs a thick layer around 180-300 μm to absorb photons [4].

The band gap of 1.1 eV for Si does not absorb more than 50% of the visible spectrums. CIGS cell efficiency and stability are comparable to Si solar cells. Recently, Tiwari group (EMPA Switzerland) reported a record efficiency of 20.4% on flexible polymer foil (23% in glass), independently confirmed by Fraunhofer Institute for Solar Energy Systems Freiburg [5]. Recently, the same group reported an efficiency of 20.8% using low temperature processing of 450°C [6]. Similar to the CIGS absorber, CdTe is also an excellent absorber material for thin film solar cells due to its ideal bandgap of ~1.5 eV.

In the TFSCs family, cuprous sulfide-cadmium sulfide ($\mathrm{Cu_2S/CdS}$) single junction is the first reported solar cell developed for space applications that showed high efficiency (~9.1%). Several start-up companies have been established to commercialize this technology but diffusion of copper into CdS matrix and doping of the CdS layer led to long-term performance degradation, for which most of the research activities on $\mathrm{Cu_2S/CdS}$ cells were declined [7]. Eventually, other genre of TFSCs took over the researchers and manufacturers interests. Among these TFSCs, amorphous silicon (a-Si) solar cell is preferable to researchers because of its material availability, non-toxicity, low processing temperature, and low cost. Meanwhile, chalcopyrite based CIGS solar cells showed comparable efficiencies to the polycrystalline Si solar cell, but the production cost of this cell is reported to be much lower than that of the polycrystalline Si solar cell. One of the major barriers in commercialization of this cell is the resource limitation, since Indium (In) and Gallium (Ga) are considered as scarce materials. On the other hand, quaternary semiconducting compound Copper Zinc Tin Sulphide (CZTS) is anatomically similar to CIGS but uses the earth-abundant elements that alleviate the material scarcity issue precluding CIGS cell potentials. Recently, a promising binary material: Cadmium Telluride (CdTe) is showing much promises due to its frequently reported higher efficiencies in comparison to polycrystalline Si solar cells [8] despite its growth nature and crystal structure is remarkably different from other p-n junction based TFSCs. As a result, CdTe received more attention than other TFSC materials as an absorber for achieving a highly efficient and low-cost solar cell. Besides, non p-n junction based DSSC cells are unique among the TFSCs in terms of structure, light absorption capacity, electron and hole transport mechanism etc. It is also a promising candidate in the TFSC technology, because of its cheap constituent materials without requiring higher purity which lowers the fabrication cost [9].

The aim of this research is to study the properties of thin films to search for the suitability of these films for the manufacture of solar cells based on $Cu(InGa)Se_2$ semiconductor material for better utilization of the solar spectrum to yield higher efficiency and performance stability. Existing issues to be solved are discussed and methods to further improve the cell performance are suggested. Future prospects of these solar cells are outlined.

2 Inception and progress

History of CIGS thin-film solar cells accounts that, the first $CuInSe_2$ (CIS) thin film was synthesized by Hahn in 1953 [10]. The very first CIS material being synthesized was in 1953, and then, an efficiency of 12% has been reported for single crystal $CuInSe_2$-based solar cells in 1974 [11]. In 1976, the first CIS thin film solar cell with buffer layer CdS was fabricated with an efficiency of 4–5% by evaporating $CuInSe_2$ powder in the presence of excess Se vapor (coevaporation) [12]. CIG-based thin film solar cell ($CuInSe_2$) started to receive even more attention in 1981 when Mickelsen and Chen achieved an efficiency of 9.4% by using a coevaporation technique from an evaporated n-type CdS atop the crystalline p- $CuInSe_2$ onto inexpensive substrates [13]. Incorporation of Ga into the CIS matrix to raise the absorber bandgap, open-circuit voltage and a fill factor led to achieve high efficiency CIGS cell fabricated by PVD of the constituent elements on the Mo-coated soda lime glass substrate. To date, NREL is a leading research organization in CIGS solar cell development. The record efficiencies of this solar cell reported by NREL were 17.1% in 1995 [14], 18.8% in 1999 [15], and 19.9% in 2008 [16]. For depositing absorber layer, glass substrate is the most commonly used substrate; however, the current trend is to develop flexible solar cells on metal foils [17-19] where by using alternative of metal foil substrates, the first report in the use of polyimide as a flexible substrate and a CIGS cell has been developed by a two-step process of sputtering metal precursors [10-22]. In 1992, the absorber layer has been deposited on flexible Mo, Ti, and Al foils by using an e-beam evaporation process with subsequent selenization [23] and state-of-the-art highest efficiency CIGS solar cells were prepared on polymer foil 2013 [24]. The efficiency champion CIGS solar cell fabricated by CIS absorber engineering and enhanced surface treatment of the absorber layer using a co-evaporation process on rigid glass substrate has been reported about 22.6% [25].

3 Crystal structure of CIGS

The I–III–VI_2 ternary compounds $CuInSe_2$ (CIS), $CuGaSe_2$ (CGS), and their alloy are well known to crystallize in chalcopyrite (ch) structure with tetrahedral bonding character [26,27]. Figure 1 depicts the chalcopyrite CIGS Crystal structure [28]. Each I(Cu) or III(In) atom has four bonds to the VI atom(Se).

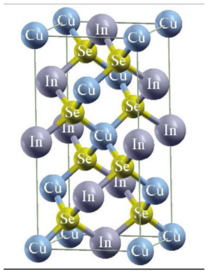

Figure 1. Tetragonal unit cell of $CuInSe_2$ [28]. Permission to use this figure has been obtained from the relevant journal.

The ternary chalcopyrites crystallize in the tetragonal structure type of space group I42d. Thus the chalcopyrite structure is a super-lattice of the Zinc Blende structure (ZnS) by doubling its unit cube along the z-axis converted to the c-axis of the chalcopyrite structure. In most real chalcopyrite crystals, the ratio of c/a is approximately equal to two, whereas in an ideal chalcopyrite structure the ratio of the unit cell length c to a is equal to two. The tetrahedral coordination implies that the bonding is primary covalent with SP^3 hybrid bonds prevalent, although there is some ionic character because the atoms are different. I–III–VI_2 compounds can be regarded as the ternary analogs of the II–VI binary compounds with some interesting structural anomalies relative to their binary nature. First, unlike their binary analogs, the ternary chalcopyrites have two different cations, e.g. ZnSe and $CuGaSe_2$. Starting from the A atom and translating it into the vertical direction through intervals of c/2, the sequence ABAB can be found, whereas horizontal translation with an interval of A, the sequence AAAA can be found. Secondly, the ratio of the lattice parameters $n = c/2a$ differs from 1 by about 2%. Thirdly, the anions are displaced from their zinc-blende sites. This reflects the fact that each cation A has four anions X as nearest neighbors in binary AX, Zinc Blende compounds, whereas in a ternary chalcopyrite ABX_2, each cation A and B has four anions X as nearest neighbors, and each anion has two A and B cations as the nearest neighbors. As a result, the anion X usually adopts an equilibrium position closer to one pair of cations than to the other, which results in unequal bond lengths $R_{AX} \neq R_{BX}$ (bond alternation). The nearest neighborhood anion–cation bond lengths are given by:

$$R_{AX} = a\left[U^2 + \frac{(1+n)^2}{16}\right]^{1/2},$$

and

$$R_{BX} = a\left[(U - (\tfrac{1}{2}))^2 + \frac{(1+n^2)}{16}\right]^{1/2}.$$

Hence, the anion displacement $U - 1/4 = (R_{AX}^2 - R_{BX}^2)/a^2$ shows the extent of bond alternation in the system. The structural anomalies n – 1 and u – 1/4 relative to the Zinc Blende structure (n = 1 and u = 1/4) are seem to be significant [29].

4 Electronic properties

Among group II-VI compound semiconductor nanoparticles, ZnS and CdS are the most promising materials. ZnS is a good material for detecting ultraviolet and violet radiation due to its primary band gap of 3.68 eV (345 nm) and high sensitivity. It has potential applications in optics, optoelectronics, and solar energy. CdS with a direct band gap of 2.42 eV (515 nm) has applications in window layers, light emitting diodes, and photodetectors. Its applications in photodetector and solar cells when used in conjunction with narrow band gap materials such as CdTe have been reported [30].

Here we describe the energy band structure and the electronic charge distribution in $CuInSe_2$ and $CuGaSe_2$, the simplest ternary analogs of II–IV zincblende compounds. The uppermost valence bands of I–III–VI_2 compounds are profoundly influenced by the proximity of noble metal d-levels in the valence band. The presence of the noble metal d-levels in the valence band has been confirmed directly by the observation of electro reflectance structure due to transitions from the d-levels themselves to the lowest conduction band minimum [31]. The energy gap is 1.3 eV less than that of the binary analog $Zn_{0.5}Cd_{0.5}Se$, and the spin-orbit parameter of 0.23 eV is considerably less than that of measured in CdSe. These two anomalies, the downshift of the energy gaps relative to the binary analogs, and reduced spin-orbit splitting have been observed to various degrees in all I–III–VI_2compounds investigated. Shay and Kasper [32] have pointed out that the anomalous reduction in the band gaps of ternary chalcopyrite related to their binary analogs are correlated with the existence of d bonding in former compounds. They found that the band gap anomaly ΔE_g correlates almost linearly with the percentage of d character, αd, deduced by comparing the spin-orbit splitting of the ternary and binary compound, i.e., $\Delta E_g = a\, \alpha\, d$ with a ≈ 3.125 eV. They have suggested that $CuInSe_2$ and $CuGaSe_2$ have a nearly constant percentage of d character (αd = 0.34 and 0.36, respectively). The I–III–VI_2 thernary compounds ($CuInSe_2$, $CuGaSe_2$, and their alloys $CuIn_xGa_{1-x}Se_2$) are promising materials for thin-film solar cells with high conversion efficiencies and low production costs [33,34].

The reason CIGS has been one of the most promising absorber layers for thin film photovoltaic devices is due to its high absorption coefficient for solar radiation and compatibility of its bandgap (1.6 eV–1.0 eV) [35]. The advantages of CIGS-based solar cells over CIS-based solar cells are as follows: (i) the bandgap can be tuned by adjusting the Ga/In ratio to match the solar spectrum. If all indium (In) is replaced by gallium (Ga), the CIGS bandgap increases from about 1.04 eV to 1.68 eV [36]. It has been stated that CIGS absorber layer can absorb most parts of the solar spectrum with a thickness of 1 μm [35]. Hence, a layer thickness of ~2.0–2.5 μm will be sufficient for the completed device, and a thinner layer device means reduction in raw material usage and lower production cost incurred. (ii) Ga incorporation can also improve the open-circuit voltage V_{oc} of CIGS since V_{oc}~E_g/2 (E_g is referring to bandgap) [37].

The electronic properties of I-III-VI2 semiconductors have been subject of study for nearly 40 years by different authors using distinct methodologies. As representative examples, we can mention the seminal work of Jaffe and Zunger where they studied self consistently within the density-functional theory (DFT), the chemical trends in the electronic structure of six Cu-based ternary chalcopyrite semiconductors including $CuGaS_2$ [34,35]. They reported 1.65 and 1.25 eV for the energy gap of $CuAlSe_2$ and $CuGaS_2$, far from the accepted experimental values 2.65 and 2.43 eV, respectively. Using full-potential linear muffin-tin orbital method based on the local-density approximation and with the Hedin and Lundqvist parametrization for the exchange and correlation potential, Ahuja et al, obtained a similar value for the energy gap of $CuGaS_2$ (1.2 eV) [38].

The first theoretical investigation of chalcopyrite semiconductors was published by Jaffe and Zunger in 1983 [38]. They calculated lattice parameters, tetragonal distortions, anion displacements, and band-structures of $CuGaS_2$, $CuInS_2$, $CuGaSe_2$, and $CuInSe_2$. In 1992, Wei, Ferreira, and Zunger used ab initio electronic structure calculations, the cluster expansion technique, and Monte Carlo simulations to calculate the order-disorder transition temperature for $CuInSe_2$ [39]. These researches support the statement that particular combination of methods can accurately describe the complex behavior of solids. In the mid-1990s, simulations were extended beyond the absorbing materials. Wei, Zhang, and Zunger looked at the $CuInSe_2$/CdS heterojunction of CIGS solar cells [40]. They calculated the band offsets for this essential part of the cell. Subsequently, Wei, and Zunger added the investigation of optical bowing parameter [41]. Gloeckler and Sites (2005) by numerical studies found that band gap grading can provide a beneficial effect on the solar cell [42]. Zhang et al. (1997,1998) published fundamental papers on defects in $CuInSe_2$[43,44]. They contain the calculation of defect levels and formation energies of defected complexes. A subsequent study by the same authors focused on the influence of Na on the electrical and structural properties of $CuInSe_2$[45]. In 1998, Wei, Zhang, and Zunger dealt with the issue of Ga addition to $CuInSe_2$ [46], providing a comprehensive picture of how Ga influences the band gap. The topic was recently revisited and extended by Huang [47]. He used computer simulations to show that a band gap of 1.5 eV should lead to the greatest efficiency and explains why record efficiency CIGS solar cells have a much lower band gap of about 1.15 eV.

The reason is that the open circuit voltage does not increase with increasing the Ga content above a gap of 1.15 eV. Lately, a lot of studies have been dedicated to grain boundaries. They seem to be important for good solar cells, because cells made from monocrystalline CIGS perform worse than polycrystalline cells [48]. In 2005, Gloeckler et al. studied the recombination of charge carriers at grain boundaries with two-dimensional simulations [49].

An important step towards cheaper solar cells would be the replacement of In and Ga by cheaper materials. In 2005, Raulot, Domain, and Guillemoles studied potential In- and Ga-free absorbers with ab initio methods [50].

Reduce the material costs, the expensive group–III elements (In and Ga) can be substituted by group–II–IV elements (Zn plus Sn) (CZTSe) i.e. sulfide counterpartCu_2ZnSnS_4 (CZTS). A1.04 eV voltage for $CuInSe_2$can be tuned from for $CuInSe_2$over 1.54 eV for $CuInS_2$ and to 1.68 eV for $CuGaSe_2$ to achieve a desired value and an enhanced current conversion efficiency [51, 52].

By using heterostructures in materials with different band gap (Table 1), the lattice constants must match to avoid dislocations/defects appearance at the interface. These dislocations/defects act as recombination centers and decrease the performances of solar cells.

Table 1. Band energy gap of thin-film absorbers.

absorber	M		Ref.
$CuInSe_2$	HSE	0.76	[53]
	GW	0.79	
	GW	1.04	
$CUIn\ _{.75}Ga_{0\ 25}Se_2$	LDA	0.8	[54]
	GGA	0.7	
$CUIn_{0.5}Ga_{0\ 5}Se_2$	LDA	0.9	[54]
	GGA	0.8	
$CUIn\ _{.25}Ga_{0\ 75}Se_2$	LDA	1.2	[54]
	GGA	0.8	
$CuGaSe_2$	HSE	1.35	[53]
	GW	1.56	
	GW	1.663	

5 Optical properties of CIGS

The study of the optical functions helps to give a better understanding of the electronic structure which can find potential applications in photoelectron devices and the semiconductor industry. The optical properties may be obtained from the complex dielectric function:

$$\mathcal{E}(\omega) = \mathcal{E}_1(\omega) + i\mathcal{E}_2(\omega). \quad (1)$$

The imaginary part of the dielectric function (ε) is calculated as follows:

$$\mathcal{E}_2^{\alpha\ \beta}(\omega) = \frac{4\,\pi^2 e^2}{\Omega} \lim_{\mathrm{q}\to 0} \sum_{\mathrm{c,v,k}} 2\mathrm{w_k}\ \delta\ (\mathrm{E_{CK}} - E_{VK} - \omega)\,\langle \mathrm{u_{ck+e_{\alpha}q}}\ |\mathrm{u_{VK}}\rangle\langle \mathrm{u_{ck+e_{\beta}q}}\ |\mathrm{u_{vk}}\rangle^*, \qquad (2)$$

where k, c, and v are the Bloch wave function vector, conduction band, and valance band respectively. $\mathrm{E_{jk}}$ is the single-electron energy state of band j in wave vector k, while $\mathrm{U_{jk}}$ is the cell periodic part of the wave function. Ω is the volume of primitive cell. $\mathrm{W_k}$ is the k-point weight, and e_{α} is the unit vector in the Cartesian coordinates system.

The real part of the dielectric function is given by the Kramers-kronig relation:

$$\mathcal{E}_1^{\alpha\ \beta}(\omega) = 1 + \frac{2}{\pi}\mathrm{p}\int_0^{\infty} \frac{\mathcal{E}_2^{\alpha\ \beta}(\omega')\,\omega'}{\omega'^2 - \omega^2 + \mathrm{i}\,\eta}\,\mathrm{d}\,\omega', \qquad (3)$$

where P is the principal value and η is an infinitesimal number. The knowledge of both the real and imaginary parts of the dielectric function make it possible to calculate other optical properties. Since the electron-optical phonon coupling is not considered in the calculations, we cannot describe the static dielectric constant $\mathcal{E}_0$. The high-frequency dielectric constant $\mathcal{E}_\infty$ is experimentally determined in the in-gap region $[\mathrm{i.e.}, \mathcal{E}_\infty \approx \mathcal{E}_1(0 << \omega << \mathrm{Eg})]$. In our calculations, this constant is determined from the dielectric function at $\mathcal{E}_1$(ω=0) and complementary also at $\mathcal{E}_1\ (\omega = \frac{E_g}{2})$. The absorption coefficient is obtained directly from the dielectric function by:

$$\alpha(\omega) = \frac{\sqrt{2}\omega}{\mathrm{c}}[\sqrt{\mathcal{E}_1(\omega)^2 + \mathcal{E}_2(\omega)^2} - \mathcal{E}_1(\omega)]^{1/2}, \qquad (4)$$

where c is the speed of light.

The maximum optical absorbance of the CIGS films was found with the films deposited on Mo substrate as compared to the other substrates. The absorption shift towards higher wavelengths may be attributed to the increase of crystallinity and growth in grain size which is already confirmed by XRD and SEM analysis. The highest transmittance value is observed for the CIGS deposited on ITO approximately 30% and for the Mo-CIGS film with lower transparency of 20%. This transparency is interconnected to the optical band gap which shows precise absorption edge to the optical band gap of the CIGS films deposited on Mo. This tendency of transmission spectra supports the AFM analysis of the films which could be attributed to the increment in the surface roughness that might occur to the influences on the transmission of the incident light due to the light scattering [55].

The average dielectric functions E(ω) generated by the GW method are shown in Fig. 2 [53]. Overall, all compounds show similar dielectric functions over a broad range of energy. The main difference is related to the variation in the energy gap and onset to absorption. This directly affects the real part of the dielectric function since a large gap usually implies a small dielectric constant.

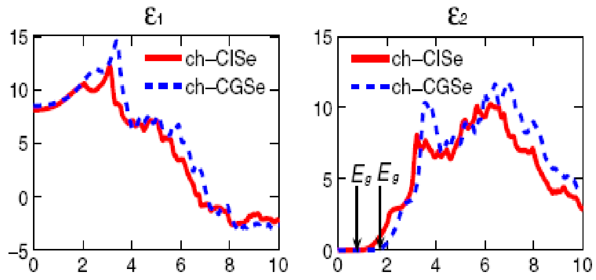

Figure 2. The average dielectric function $\mathcal{E}(\omega) = [2\mathcal{E}^{\perp}(\omega) + \mathcal{E}^{||}(\omega)]/3$ obtained from the GW calculation. Overall, CISe, and CGSe have all rather similar spectra. The high-frequency dielectric constant $\mathcal{E}_\infty$ depends on the energy gap Eg, and materials with large gap have a small dielectric constant [53]. Permission to use this figure has been obtained from the relevant journal.

The high-frequency dielectric constants $\mathcal{E}_\infty$ are presented in Table 2 in terms of transverse (⊥) and longitudinal (||) components with respect to the crystalline c-axis, in comparison with earlier calculated [56] and experimental results [57,58]. The GW dielectric constants support EV+QP results for CISe and CGSe. Approximately, all the three theoretical approaches tabulated in Table 2 give the same size order of dielectric constants. The difference between $\mathcal{E}_\infty^{\perp}$ and $\mathcal{E}_\infty^{||}$ demonstrates the existence of an anisotropy in the dielectric functions which is induced by the anisotropy of the crystalline structures. The stannite structure shows stronger anisotropy $\mathcal{E}_\infty^{\perp}/\mathcal{E}_\infty^{||} < 1$ compared with the corresponding kesterite structure.

In Fig. 3 the GW absorption coefficients are displayed. CISe has larger optical absorption coefficients than CGSe in the energy range below 2.5 eV. However, materials with absorption starting from 1.5 eV (e.g., CGSe) should be more absorbing materials in solar cells. The GW results demonstrate that the absorption peak of CZTS in energy range of the visible spectrum (1.8–3.1 eV) is a beneficial property for photovoltaic applications [33].

Table 2. The high-frequency dielectric constant $\mathcal{E}_\infty = \mathcal{E}_1(0)$ is determined by excluding the electron–phonon interaction. We also present the dielectric function at $\mathcal{E}_1$(ω=Eg/2) in the brackets. The transverse (⊥) and longitudinal (‖) components refer to the crystalline c-axis.

	ch-CISe	ch-CGSe	ke-CZTS	Ref.
$\mathcal{E}_\infty^{\perp}$	HSE	8.18 (8.29)	7.31 (7.45)	[23]
	GW	8.26 (8.37)	8.51 (8.72)	[53]
	EV+QPa	8.2	7.6	[56]
	Expt.b	7.8, 6.86	5.13	[57,58]
$\mathcal{E}_\infty^{\parallel}$	HSE	7.62 (7.69)	7.25 (7.39)	[53]
	GW	7.83 (7.92)	8.42 (8.64)	[33]
	EV+QPa	7.8	7.5	[56]
	Expt.b	7.8, 6.0	4.2	[57,58]

a Refs. [56]: a GGA potential plus a quasi-particle correction of the band gap.

b Refs. [57] and [58]: experimental results.

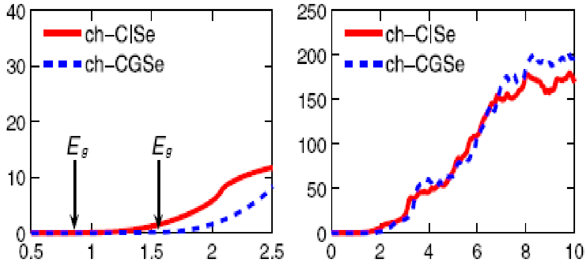

Figure 3. The optical absorption coefficient α(ω) is obtained directly from the GW dielectric functions in scheme 3 using Eq. (3). We show both the absorption close to the visible spectrum (left panels) and in a broader energy region (right panels) [53]. Permission to use this figure has been obtained from the relevant journal.

6 Cell materials, configuration and fabrication procedure

The active materials of CIGS solar cells are composed of direct band gap tetrahedrally bonded compound-element semiconductors having a chalcopyrite crystal structure. Figure 4 shows the typical structure of a CIGS solar cell, indicating some commonly used materials for the different layers. A more detailed description is available else-where [59–62]. The most commonly used substrate is rigid, 3-4 mm thick soda-lime glass (SLG), as it is thermally stable, chemically inert, has a similar thermal expansion coefficient as the absorber. It also has a smooth surface, insulating properties suitable for monolithic interconnection and can supply alkali elements for high efficient cells (see section "Alkali post deposition treatment of CIGS layer"). However a significant amount of work has also been done for CIGS on flexible substrates such as metal foils, ceramics and polymer films, as discussed in more detail elsewhere [60].

The preferred back contact consists of sputtered molybdenum, serving as a quasi-ohmic contact with the absorber by formation of a $MoSe_2$ intermediate layer during absorber growth. The p-type CIGS absorber can be grown by co-evaporation processes, with selenization followed by sulfurization of precursors deposited by sputtering, electrodeposition, or printing. While co-evaporation led to the highest efficiencies for a long time [61–63], the largest commercial manufacturer and current world record holder Solar Frontier is using a sputtered precursor with subsequent selenization and sulfurization which reported a record efficiency of 22.3% [64,66]. Various CIGS compositions are used, mainly aiming at tuning the material band gap (In-Ga ratio, Se-S ratio), as well as its bulk and surface electronic properties. Among others, the introduction of a band gap grading and the presence of alkali elements are two key features that have fueled the development of higher efficiencies in recent years.

Generally, CIGS solar cells are grown in a substrate configuration. This configuration provides the highest efficiency owing to favorable process conditions and material compatibility but requires an additional encapsulation layer and/or glass to protect the cell surface. This covering glass, in contrast, is not required for the cells grown in the superstrate configuration. CIS-based superstrate solar cells were investigated by Duchemin et al. [67] using spray pyrolysis deposition, but the efficiencies did not exceed 5%. CdS/CIGS superstrate cells do not provide the desirable interdiffusion of Cd into CIS (or CIGS) during high temperatures required for absorbing deposition on CdS buffer layers [68].

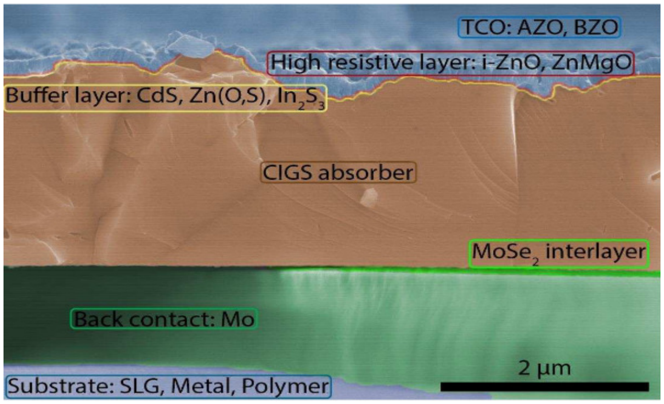

Figure 4. Schematic diagram of a typical CIGS solar cell, with examples of the most commonly used materials [62]. Permission to use this figure has been obtained from the relevant publication.

The main reason for this low efficiency in CdS/CIGS superstrate cells is the undesirable interdiffusion of Cd in to CIS (or CIGS) during the elevated temperatures required for absorber deposition on CdS buffer layers [68]. To overcome this problem of interdiffusion more stable buffer materials and low-temperature deposition processes such as electrodeposition (ED), low-substrate temperature coevaporation, and screen printing were investigated. Nakada and Mise [69] achieved a breakthrough by replacing CdS with undopped ZnO and coevaporating Na_xSe during CIGS deposition. With the additional introduction of composition grading in absorber layer, 12.8% efficiency cells were developed [70].

Numerous simulation and experimental studies have been performed in the photovoltaic field to obtain high conversion efficiency and to increase the stability and durability of the technology. The evolution from 6% efficient crystalline silicon (c-Si) cell is reached to 25.0% [69]. The emergence of new materials, and the new concept boost the efficiency up to 44.7 % for multi-junction (tandem four junction) solar cell [71]. For chalcopyrite thin-film solar cells, in CIGS the experimental and simulation results for different combination have been compared in a recent work [72]. The efficiency for CIGS has obtained an efficiency of 20.8 % for 1 sun but it is 22.8% for concentrated solar cell applications [73].

The CIGS film consists of a p-CIGS absorber layer with combination of n-CdS layer and ZnO window layer. The band gap here is a function of Gallium and can be varied from 1.0 – 1.67 eV, that would cause the effect in the variation of other solar cell parameters [74]. Simulation results giving efficiencies above 25% are also published. Though its efficiency is high but still it is difficult to commercialize due to the availability of resources in addition to particularly rare metals, Indium (In) and gallium (Ga), that adds to the costs of the CIGS based technology [75].

Addition of alkali elements, especially Na, has long been subject of studies in the chalcopyrite thin film community, due to the beneficial impact on the electronic properties of the absorber and solar cells. If not diffusing directly from the glass substrate during the absorber deposition at elevated temperatures [76], similar beneficial effect on the bulk electronic properties were observed when adding them in a controlled manner prior, during, or after CIGS growth [77]. Whereas Na long showed the most beneficial effect, the controlled addition of KF in a post-deposition treatment (PDT) yielded a significant improvement in efficiency up to a world record efficiency of 20.4% [63]. Such a PDT treatment was originally found to be the most beneficial method to add Na onto CIGS grown at low-temperature on plastic substrates [78], because it allows separating the influence of Na on CIGS film growth from its beneficial effect on electronic properties.

While it was found that Na PDT mainly modifies the bulk electronic properties of the CIGS layer, with no discernible surface modification, addition of KF in a similar PDT treatment leads to a significant alteration of the CIGS surface composition, namely Cu and Ga depletion. Furthermore, a decrease in Na content for samples treated with K is also systematically observed [63, 79], possibly based on an ion exchange mechanism. The modified CIGS surface has strong implications on the interface formation and growth of subsequent layers, especially when grown by chemical bath methods [63, 64]. A review of the impact of addition of KF after the growth of CIGS is presented in ref. [63]. Strengthened by several consecutive world records for the CIGS technology when applying a process based on alkali-addition after CIGS growth [63,64], these findings shed new light on the importance of considering the alkali addition process together with alkali type and their combination and the effects on both bulk as well as surface/interface properties of CIGS and solar cells. Whether the effect of KF PDT is a direct electronic effect due to the modified surface composition of the CIGS layer or whether it indirectly affects the junction quality by modifying the interface properties during buffer layer deposition is still under discussion. Influence on the bulk properties are also to be considered and cannot be excluded from the overall effects on solar cell efficiency [80].

CIGS thin film technology has been mostly developed on glass substrates, and for a long time CIGS solar cells deposited on flexible substrates such as plastic films or metal foils could not reach similar efficiencies. Limitations due to impurity diffusions or the need for lower growth temperatures imposed by the choice of the substrate were reasons for such efficiency gap. Recent developments [80] however showed that those challenges can be overcome, and is best exemplified with an efficiency above 20% achieved on polyimide (PI) foil. Deposition on a flexible substrate has advantages not only for manufacturing (large area roll-to-roll deposition is possible), but opens up a whole new field for solar module designs and applications. Especially, flexible and lightweight CIGS solar modules enable novel applications and concepts for solar electricity generation. Flexibility in shape, power rating, and form factor are some of the advantages that allow clear differentiation from traditional rigid and heavy PV technologies, opening the doors to BIPV and TIPV markets. Beside full flexible solar modules, BIPV solutions can be provided by laminating lightweight solar modules directly onto metallic building elements. Significant reduction of BOS, transport and installation cost can be expected compared to conventional glass-glass technologies.

The Gallium concentration was changed and the effect of different parameters were observed in the CIGS thin film solar cell; the summary of results were tabulated in Table 4. The open circuit voltage (Voc) and the band gap of the CIGS layer increases as the gallium (Ga) content increases. The short circuit current represented by (J_{SC}) decreases as the band gap increases due to the recombination of carriers, thus it has the reverse effect then Voc. Similarly, the Fill-Factor (FF) increases up to 50%, moreover, due to an increase in Ga contents beyond 50% which causes decrease in FF, the same phenomenon is also observed in the case of external quantum efficiency η (%). By increasing η up to 66% of Ga contents, further increase of Ga causes decrease in η [73]. The summary of result obtained by using scaps (solar cell capacitance simulator) are demonstrated in Table 3 [81].

Table 3. Photovoltaic parameters for CIGS solar cells with different Ga content [81].

Ga content	Method	Voc (V)	Jsc (mA/cm2)	FF (%)	eta (%)
0.00	scaps	0.5282	48.3933	79.75	20.38
0.31	scaps	0.6747	46.2690	82.37	25.71
0.45	scaps	0.7733	45.7018	83.43	29.48
0.66	scaps	0.8768	42.0037	84.04	30.0
1.00	scaps	0.8807	38.5823	83.59	28.40

Eta: Estimated Time Of Arrival

7 Results and discussion

To date, CIGS cells have comparable efficiencies to the polycrystalline Si solar cell. These cells could be deposited on both rigid glass substrates or flexible substrates and it was observed that the efficiency is higher when the cell is deposited on rigid substrates, i.e., soda lime glass substrate due to the positive effect of Na. In Fig. 6, two separate efficiency lines can be seen for the CIGS solar cell, one is based on a rigid substrate (R) and another is for a flexible substrate (F). Notice that the efficiency of CIGS cells deposited on a flexible substrate gradually progresses towards the cell deposited on a rigid substrate. It is already mentioned that the manufacturing cost of this cell is lower than that of crystalline solar cell but scarcity of In and Ga is still the vital challenge. Most of the buffer layer of CIGS contain toxic cadmium content is another bottleneck that limits the potential of this solar cell. Similar to (CIGS), the CdTe is one of the most investigated materials among the second generation thin film solar cells. However, there are some issues regarding the cost of raw materials. Toxicity. CZTS is another promising thin film solar cell which is anatomically similar structured like CIGS. That is, fabrication procedure of different layers such as buffer, window, and TCO layer of CZTS is also similar to the CIGS cell. Beside these, DSSC cells are unique among the TFSCs in terms of cell structure and constituent materials. This solar cell is the promising likewise of CZTS because of earth abundance of its constituent elements and their environmentally benign nature. Therefore, CZTS is one of the most desirable and adorable PV materials despite its' reported efficiency is lower compared to CIGS and CdTe. A summary of the five TFSCs research works has been presented in Table 6 as a comparative data for structural, optical, and electrical properties, material availability, toxicity, stability, and highest efficiency.

Thin-film solar cells cover around 4.5% of worldwide photovoltaic market share where a-Si:H covered 0.3%, CIGS covered 1.9%, and CdTe covered 2.3% of the market share in 2018. Both CIGS and CdTe solar cell enjoy the advantage of their matured fabrication technology, presently their efficiency is comparable with multicrystalline silicon solar cells but their cost is comparatively lower than this type of Si solar cells. Both of these cells can be deposited on either rigid glass substrates or flexible glass substrates, both can be configured in either superstrate or substrate stacks. However, both of them use scarce and toxic materials which are the major limitations of these cells. Again, efficiency of a-Si:H is relatively lower in comparison with CIGS and CdTe.and reduced after a certain time. In contrast, CZTS and DSSC are most promising solar cells in the thin film family, because of raw materials' abundance, environmentally benign nature, low- cost as well as easy to synthesis and processing techniques. These solar cells are still in the research and development phase, so its market share is not mentionable but their progress is slowly moving forward for commercializing in global PV markets.

7 Conclusions

In this article, remarkable development, constituent cell materials, fabrication procedures of major types of thin film solar cells have been reviewed. Modification of the layers in cell configuration from the primitive cell to the state-of-theart cell has been discussed with possible inclusion of new raw materials and fabrication processes. Limitations for which performance of these cells that are still below market-dominant silicon solar cell have also been discussed. The record efficiency, to date, for a-Si:H, CIGS, CZTS, CdTe, and Dye sensitized solar cell (DSSC) is 13.4%, 22.5%, 12,6%, 22.1%, and 15% respectively. Among them, CZTS and DSSC are still in research and development phase while the efficiencies of CIGS and CdTe solar cell are comparable with the c-Si solar cells efficiency. However the manufacturing process of c-Si cell poses more challenges than thin film solar cells. So, thin film PV technologies are believed to be the most promising for terawatt scale PV deployment among the existing renewable energy technologies that could mitigate present as well as future energy crisis. Therefore, extensive research efforts must be given to overcome the critical issues related to the TFSCs for popularization as well as for viable commercialization.

References

[1] M. Jamiati, B. Khoshnevisana, M. Mohammadib, "Second- and third-order elastic constants of kesterite CZTS and its electronic and optical properties under various strain rates." Energy Sources, Part A: Recovery, Utilization, and Environmental Effects, **40** (2018) 977.

[2] A. Kowsar, S. F. U. Farhad, "High Efficiency Four Junction III-V Bismide Concentrator Solar Cell: Design, Theory, and Simulation." International Journal of Renewable Energy Research (IJRER), 8 (2018) 17621769.

[3] D. Jeyakumar Ramanujama, et al., "Flexible CIGS, CdTe and a-Si:H based thin film solar cells: A review." Progress in Materials Science, **110** (2020) 100619.

[4] R. Light, "Trapping in thin silicon solar cells: A review on fundamentals and technologies." Progrees in photovoltaics, **7** (2021) 3440.

[5] C. Romain, et al., "Advanced alkali treatments for high-efficiency Cu(In,Ga)Se_2 solar cells on flexible substrates." Advanced Energy Materials, **9** (2019) 1900408.

[6] A. Bosio, S. Pasini, N. Romeo, "The History of Photovoltaics with Emphasis on CdTe Solar Cells and Modules." Advances in Thin Films for Photovoltaic, **10** (2020) 344.

[7] Y. Wu, et al., "Synthesis and photovoltaic application of copper (I) sulfide nanocrystals."

Nano letters, **8** (2008) 2551.

[8] M. A. Green, et al., "Solar cell efficiency tables (version 52)." Progress in Photovoltaics: Research and Applications, **26** (2018) 427.

[9] A. Kowsar, et al., " Progress in Major Thin-film Solar Cells: Growth Technologies, Layer Materials and Efficiencies." International Journal of renewable energy research, **9** (2019) 579.

[10] U. Rau, H. W. Schock, "Cu(In,Ga)Se_2 solar cells," in Clean Electricity from Photovoltaics, ed: World Scientific, (2001) 277-345.

[11] S. Wagner, J. Shay, P. Migliorato, H. Kasper, "$CuInSe_2$/CdS heterojunction photovoltaic detectors." Applied Physics Letters, **25** (1974) 434.

[12] L. L. Kazmerski, F. R. White, G. K. Morgan, “Thin-film $CuInSe_2$/CdS heterojunction solar cells.” Applied Physics Letters, **29** (1976) 268.

[13] R. Mickelsen, W. Chen, "Development of a 9.4% efficient thin-film $CuInSe_2$/CdS solar cell." in 15th photovoltaic specialists conference, (1981) 800.

[14] J. Tuttle, et al., "Accelerated publication 17.1% efficient Cu(In,Ga) Se_2- based thin- film solar cell." Progress in Photovoltaics: Research and Applications, **3** (1995) 235.

[15] M. A. Contreras, et al., "Progress toward 20% efficiency in Cu (In, Ga) Se_2 polycrystalline thin- film solar cells." Progress in Photovoltaics: Research and applications, **7** (1999) 311.

[16] I. Repins, et al., "Characterization of 19.9%efficient CIGS absorbers." Photovoltaic Specialists Conference, 2008. PVSC'08. 33rd IEEE, (2008) 1-6 .

[17] T. Satoh, et al., "Cigs solar cells on flexible stainless steel substrates," in Photovoltaic Specialists Conference, 2000. Conference Record of the Twenty-Eighth IEEE, (2000), 567-570 .

[18] R. Wuerz, et al., "CIGS thin-film solar cells on steel substrates." Thin Solid Films, **517** (2003) 24152418.

[19] C. Shi, et al., "Cu(In,Ga)Se_2 solar cells on stainless-steel substrates covered with ZnO diffusion barriers." Solar Energy Materials and Solar Cells, **93** (2009) 654.

[20] B. M. Başol, et al., "Flexible and light weight copper indium diselenide solar cells on polyimide substrates," Solar Energy Materials and Solar Cells, **43** (1996) 9398.

[21] M. Feli, F. Parandin, "A Numerical Optimization of an Efficient Double Junction InGaN/CIGS Solar Cell." Journal of Electrical. Computer Engineering Innovations, **6** (2018) 53.

[22] H. Zachmann, et al., "Characterisation of Cu(In,Ga)Se_2-based thin film solar cells on polyimide." Thin Solid Films, **517** (2009) 2209.

[23] B. M. Başol, et al., "Copper indium diselenide thin film solar cells fabricated on flexible foil substrates." Solar Energy Materials and Solar Cells, **29** (1993) 163.

[24] M. A. Green, et al., "Solar cell efficiency tables (version 42)." Progress in Photovoltaics: Research and Applications, **5** (2013) 827.

[25] Michael Powalla, et al., "Advances in Cost-Efficient Thin-Film Photovoltaics Based on Cu(In,Ga)Se_2." Engineering, **3** (2017) 445.

[26] J. Parkes, R. D. Tomlinson, M. J. Hampshire, " Crystal data for $CuInSe_2$." Journal of Applied Crystallography, **6** (1973) 414.

[27] S. C. Abrahams, J. L. Bernstein, "Piezoelectric nonlinear optic $CuGaSe_2$ and $CdGeAs_2$: Crystal structure, chalcopyrite microhardness, and sublattice distortion." Journal of Chemical Physics, **61** (1974) 1140.

[28] S. Chen, X. G. Gong, S. H. Wei, "Band-structure anomalies of the chalcopyrite semiconductors $CuGaX_2$ versus $AgGaX_2$ (X=S and Se) and their alloys." Physical Review B, **75** (2007) 205209.

[29] C. D. R. Ludwig, T. Gruhn, C. Felser, " Indium-Gallium Segregation in CuInxGa1-xSe_2: An Ab Initio-Based Monte Carlo Study." Physical Review Letters, **105** (2010) 025702.

[30] J. Osuntokun, P. A. Ajibade, "Structural and Thermal Studies of ZnS and CdS Nanoparticles in Polymer Matrices." Journal of Nanomaterials, **2016** (2016) 3296071.

[31] J. L. Shay, H. M. Kasper, L. M. Schivone, "Electronic Structure of $AgInSe_2$ and $CuInSe_2$." Physical Review B, **7** (1973) 4485.

[32] J. L. Shay and H. M. Kasper, " Direct Observation of Cu-d Levels in I-III-VI2 Compounds." Physical Review Letters, **29** (1972) 1162.

[33] U. Rau, K. Taretto, S. Siebentritt, "Grain boundaries in $Cu(In,Ga)(Se,S)_2$ thin-film solar cells." Applied Physics A, **96** (2009) 221.

[34] P. Palacios, et al., "Thermodynamics of the Formation of Ti- and Cr-doped $CuGaS_2$ Intermediate-band Photovoltaic Materials." Journal of Physical Chemistry C, **112** (2008) 9525.

[35] T. D. Lee, A. Ebong, “Thin film solar technologies: a review.” in 2015 12th International Conference on High-capacity Optical Networks and Enabling/Emerging Technologies (HONET), Islamabad, Pakistan, December 2015, (2015) 1.

[36] Y. C. Wang, H. P. D. Shieh, “Double-graded bandgap in $Cu(In,Ga)Se_2$ thin film solar cells by low toxicity selenization process.” Applied Physics Letters, **105** (2014) 073901.

[37] J. Ramanujam, U. P. Singh, “Copper indium gallium selenide based solar cells – a review.” Energy & Environmental Science, 10(6) (2017) 1306.

[38] J. E. Jaffe, A. Zunger, “Electronic structure of the ternary chalcopyrite semiconductors $CuAlS_2$, $CuGaS_2$, $CuInS_2$, $CuAlSe_2$, $CuGaSe_2$, and $CuInSe_2$." Physical Review B, **28** (1983) 5822.

[39] S. H. Weiand, L. G. Ferreira, A. Zunger, "First-principles calculation of the order-disorder transition in chalcopyrite semiconductors." Physical Review B, **45** (1992) 2533.

[40] S. H. Weiand, A. Zunger, " Band offsets at the CdS/CuInSe2 heterojunction." Applied Physics Letters, **63** (1993) 2549.

[41] S. H. Weiand, A. Zunger, "Band offsets and optical bowings of chalcopyrites and Zn-based II-VI alloys." Journal of Applied Physics, **78** (1995) 3846.

[42] M. Gloeckler, J. R. Sites, "Guidelines for Optimization of the Absorber Layer Energy Gap for High Efficiency $Cu(In,Ga)Se_2$ Solar Cells." Journal of Physics and Chemistry of Solids, **66** (2005) 1891.

[43] S. B. Zhang, S. H. Weiand, A. Zunger, "Stabilization of Ternary Compounds via Ordered Arrays of Defect Pairs." Physical Review Letters, **78** (1997) 4059.

[44] S. B. Zhang, S. H. Weiand, A. Zunger, H. Katayama-Yoshida, " Defect physics of the CuInSe2 chalcopyrite semiconductor." Physical Review B, **57** (1998) 9642.

[45] S. H. Weiand, S. B. Zhang, and A. Zunger, "Effects of Na on the electrical and structural properties of $CuInSe_2$." Journal of Applied Physics, **85** (1999) 7214.

[46] S. H. Weiand, S.B. Zhang, and A. Zunger, "Effects of Ga addition to $CuInSe_2$ on its electronic, structural, and defect properties." Applied Physics Letters, **72** (1998) 3199.

[47] C. H. Huang, "Effects of Ga content on $Cu(In,Ga)Se_2$ solar cells studied by numerical modeling." Jornal of Physics and Chemistry of Solids, **69** (2008) 330.

[48] Z. A. Shukri, et al., "Preliminary photovoltaic cells with single crystal CIS substrates." Solar Energ. Mater. and Solar Cells, **37** (1995) 395.

[49] M. Gloeckler, J. R. Sites, W. K. Metzger, "Grain-boundary recombination in $Cu(In,Ga)Se_2$ solar cells." Journal of Applied

Physics, **98** (2005) 113704.

[50] J. M. Raulot, C. Domain, J.F. Guillemoles, "Ab initio investigation of potential indium and gallium free chalcopyrite compounds for photovoltaic application." Journal of Physics and Chemistry of Solids, **66** (2005) 2019.

[51] W. N. Shafarman, S. Siebentritt and L. Stolt, Handbook of Photovoltaic Science and Engineering, Wiley, New York (2011).

[52] P. Jackson, et al., "High quality baseline for high efficiency, $Cu(In_{1-x},Gax)Se_2$ solar cells." Progress in Photovoltaics: Research and Applications, **15** (2007) 507.

[53] H. Zhao, C. Persson, "Optical properties of $Cu(In,Ga)Se_2$ and $Cu_2ZnSn(S,Se)_4$." Thin Solid Films, **519** (2011) 7508.

[54] M. Chandramohan, S.Velumani, T. Venkatachalam, "Band structure calculations of $Cu(In_{1-x}Gax)Se_2$." Journal of Materials Science and Engineering B, **174** (2010) 200.

[55] A. Bouich, et al., " Deposit on different back contacts: to high-quality $\mathrm{Cu(InGa)S_2}$ thin films for photovoltaic application." Journal of Materials Science: Materials in Electronics, **30** (2019) 20832.

[56] C. Persson, "Electronic and optical properties of Cu2ZnSnS4 and Cu2ZnSnSe4." Journal of Applied Physics, **107** (2010) 053710.

[57] T. Kawashima, et al., "Optical constants of CuGaSe2 and $CuInSe_2$." Journal of Applied Physics, **84** (1998) 5202.

[58] N. N. Syrbu, et al., "Lattice vibrations in $\mathrm{CuIn_{(1-x)}Ga_xSe_2}$ crystals." Journal of Physics B, **229** (1997) 199.

[59] F. Ghavami, A. Salehi, "High-efficiency CIGS solar cell by optimization of doping concentration thickness and energy band gap." Modern Physics Letters B, 34(4) (2020) 2050053.

[60] P. Reinhard, et al., "Review of Progress Toward 20% Efficiency Flexible CIGS Solar Cells and Manufacturing Issues of Solar Modules." IEEE Journal of Photovoltaics, **3** (2013) 572.

[61] W. N. Shafarman, S. Siebentritt, L. Stolt, " $Cu(InGa)Se_2$ solar cells in: Luque A, Hegedus S," Handbook of photovoltaic science and engineering, England: John Wiley & Sons Ltd; pp. 546-599 (2010).

[62] R. Scheer, H. W. Schock, " Chalcogenide Photovoltaics: Physics, Technologies and Thin Film Devices." John Wiley & Sons Ltd; pp. 154-172 (2011).

[63] A. Chirilă, et al., " Potassium-induced surface modification of $\mathrm{Cu(InGa)S_2}$ thin films for high efficiency solar cells." Nature Materials, **12** (2013) 1107.

[64] T. Feurer, et al., "Progress in Thin Film CIGS Photovoltaics – R&D, Manufacturing and Applications." Progress in Photovoltaics, **25** (2017) 645.

[65] K. Kushiya, "CIS-based thin-film PV technology in solar frontier K.K " Solar Energy Materials and Solar Cells, **122** (2014) 309.

[66] " Solar Frontier Achieves World Record Thin-Film Solar Cell Efficiency : 22.3%." Solar Frontier company webpageDecember 8, 2015 Accesed April 25, 2016. http://www.solar-frontier.com/eng/news/2015/C051171.html.

[67] S. Duchemin et al., in: Photovoltaic Solar Energy. Proc. 8th European Conference, pp. 1038- 1042, Florence, Italy, (1988).

[68] T. Nakada et al., Photovoltaic Energy Conversion. IEEE First World Conference, pp. 95-98, Hawaii, USA (1994).

[69] M. A. Green, "The path to 25% silicon solar cell efficiency: History of silicon cell evolution." Progr. in Photovolt.: Research and Applications, **17** (2009) 183.

[70] T. Nakada, T.Mise, "High-efficiency superstrate type cigs thin film solar cells with graded bandgap absorber layers." Proceedings of the 17th European Photovoltaic Solar Energy

Conference, pp. 1027–1030, Munich, Germany (2001).

[71] F. Dimroth, et al., "Wafer bonded four-junction GaInP/GaAs//GaInAsP/GaInAs concentrator solar cells with 44.7% efficiency." Progr. in Photovolt.: Research and Applications, **22** (2014) 277.

[72] S. Keshmiri, H. S. Sharbati, "Model for increased efficiency of CIGS solar cells by a stepped distribution of carrier density and Ga in the absorber layer." Science China: Physics, Mechanics and Astronomy, **56** (2013) 1533.

[73] P. Jackson, et al., "Compositional investigation of potassium doped Cu(In,Ga)Se2 solar cells with efficiencies up to 20.8%." Physica Status Solidi (RRL)-Rapid Research Letters, **8** (2014) 219.

[74] H. Ullah, B. Mari, H. N. Cui, "Investigation on the Effect of Gallium on the Efficiency of CIGS Solar Cells through Dedicated Software." Applied Mechanics and Materials, **448** (2014) 1497.

[75] M. Tawheed Kibria, et al., "A Review: Comparative studies on different generation solar cells technology." Proceedings of 5th International Conference on Environmental Aspects of Bangladesh [ICEAB 2014].

[76] J. Hedstrom, et al., "Zno/Cds/Cu(in,Ga)Se_2 Thin-Film Solar-Cells with Improved Perfornance." Conference Record of the Twenty Third Ieee Photovoltaic Specialists, (1993) 364.

[77] D. Rudmann, et al., "Sodium incorporation strategies for CIGS growth at different temperatures." Thin Solid Films, **480** (2005) 55.

[78] D. Rudmann, et al., " Efficiency enhancement of Cu(In,Ga)Se_2 solar cells due to post deposition Na incorporation." Applied Physics Letters, **84** (2004) 1129.

[79] P. Reinhard, et al., " Features of KF and NaF Postdeposition Treatments of Cu(In,Ga)Se2 Absorbers for High Efficiency Thin Film Solar Cells." Chemistry of Materials, **27** (2015) 5755.

[80] L. M. Mansfield, et al., " Enhanced Performance in Cu(In,Ga)Se Solar Cells Fabricated by the Two-Step Selenization Process With a Potassium Fluoride Postdeposition Treatment." IEEE Journal of Photovoltaics, **4** (2014) 1650.

[81] H. Ullah, B. Marí, L. M. Sánchez Ruiz, "Comparative analysis of CIGS thin film and Multilayer Solar cells." Proc.Int. Conf. Engineering Education and research, Riga, Latviya, ICEE/ICIT (2014) 103.